



ACCURACY OF THE BIM MODEL GENERATED FROM THE POINT CLOUD FOR AN OBJECT MADE IN GLASS TECHNOLOGY

Marta Wider, Pelagia Gawronek

Summary

Mapping glass objects in 3D space has long raised doubts as to the possibility of obtaining data, and as to the accuracy of that data. The basics of terrestrial laser scanning technology and the principles of the physics of light propagation in the environment of transparent and reflective surfaces, as a rule, contradict the technological possibility of a faithful mapping thereof. Although Building Information Modelling (BIM) of existing objects based on data from terrestrial laser scanning is an increasingly common practice, it is recognized, nevertheless, that the accuracy of the model is primarily reflected in the accuracy of the point cloud obtained as a result of scanning. The article discusses the possibilities of developing a BIM model of an object made in glass technology, based on data obtained with the method of terrestrial laser scanning. The subject of the study was the glazed façade of the complex of buildings belonging to the University of Agriculture in Krakow. The study on the fidelity of mapping glazed surfaces included the acquisition and processing of the point cloud, 3D modelling of the object using the Revit software, and the analysis of the accuracy of mapping the existing status in comparison with architectural design and construction documentation. Based on the research, the possibility of using the BIM process was assessed using TLS data in the process of recreating the geometry of an object made in glass technology. The results of the study showed a significant convergence of the façade model geometry with the actual course of the structure, which, however, can be attributed to the development methodology, i.e. the accuracy of 3D data acquisition, the registration process, the filtration procedure, the method of parametric modelling of the façade structure itself, and ultimately fitting three-layer glazing into the model of that structure.

Keywords

terrestrial laser scanning • architectural survey • modelling • glass façade • accuracy analysis of geometry modelling

1. Introduction

According to the *Budownictwo. Innowacje. Wizja liderów branży 2025* [Construction industry. Innovations. 2025 Vision of Industry Leaders], developed in 2019 by the

Centrum Badań i Analiz Rynku ASM [ASM Market Research and Analysis Centre] and commissioned by the Autodesk, BIM is currently the main direction of development in the construction industry [Autodesk 2019 Report]. The use of dynamically developing, modern, non-invasive measurement tools and technologies – such as terrestrial laser scanning, which enables faithful reproduction of the real geometry of objects [Głowacka and Pluta 2015, Piech et al. 2018, Kwinta and Gradka 2021] – facilitates harnessing the potential of BIM in the context of existing buildings [Baik 2017]. In the performance of object surveys with the use of BIM, the selection of technologies for acquiring spatial data becomes of fundamental importance [Alshawabkeh et al. 2021]. An important role is also played by the accuracy criteria for the formulation of the final model [Graham et al. 2018, Khosakitchalart et al. 2019]. Other significant issues include cost-effectiveness of applying the given measurement method, or time constraints related to the timing of the measurement [Kelly et al. 2013].

Despite the fact that laser scanning is considered to be one of the most accurate technologies for obtaining spatial data [Pitkänen et al. 2021], the instrument in question still encounters various limitations and difficulties. One of the most problematic in this respect is the measurement of elements made in glass technology [Kuzina and Rimshin 2017]. Recording TLS data of glass surfaces, which are transparent barriers, remains problematic [Yang 2019]. When a light beam passes through the border of transparent media, some of the ray components are reflected, and the rest passes through and gets refracted, and then, when it hits another border (the outer coating of the glass), the phenomenon repeats itself [Kamusiński 2005]. With each successive passage through the boundary, the wave weakens and gradually disappears. The laser light wave may also be subject to the phenomenon of Total Internal Reflection. In that case, a situation occurs where the beam is completely ‘trapped’ within it [Kusznier 2015]. If this happens when scanning the glass, theoretically the beam will not return to the scanner at all. The basic physics of light leads to the conclusion: all transparent barriers, even if they cause the emitted laser beam to return to the device, will be recorded with an error in the form of a shift or a distortion, and therefore in the manner not faithfully reflecting reality. The data obtained in this way cannot be used in modelling. Due to the errors obtained as a result of ray distortion, each such partition apparently mapped by the scanner should be considered false in its entirety, and therefore, as measurement noise, it should be rejected and eliminated at the point cloud filtration stage.

The problem related to the scanning of glazed surfaces has been described, among others, in the studies by Bernat et al. [2016], or Kuzina and Rimshin [2017]. The results indicated that the quality of the modelling of objects made of glass depends on the physical characteristics of the latter, its colour, roughness, or even on whether it is covered with dust and to what degree. Thick and dark panes of glass, with a rough structure, covered with a layer of dust, reflect the 3D space with the correct geometry, allowing for unambiguous identification. The surfaces of ‘clean’ glass are modelled with a significant error, and noise is generated during the measurement, which is often decisive for rejecting the point clouds of such objects in the context of an architectural

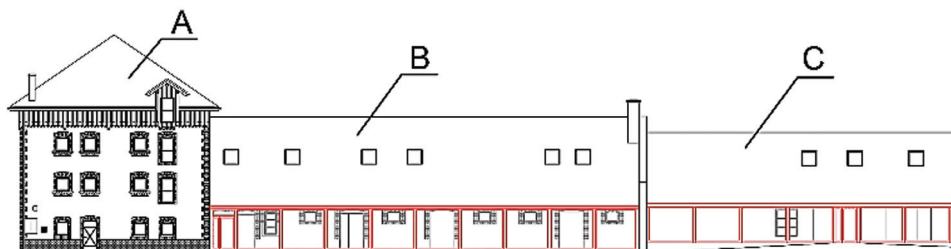
survey, for instance. Therefore, it should be assumed that the mapping of transparent surfaces on the basis of data in the form of a point cloud should be performed in a way that reflects reality most closely, in accordance with the level of accuracy adopted in the given study. For this purpose, the typical approach is to place the glass plane within the bounds of metal joinery or woodwork of the window (or door) correctly registered by the scanner, and in the case of curtain walls and other glass partitions, within the context of the glass pane's fixing structure (e.g. in the form of the so-called muntins) [Pu and Vosselman 2007].

The problem of a faithful reconstruction of the object's glazing in a three-dimensional space inspired the authors to examine the accuracy of the BIM model developed from the point cloud of the glass façade of a historic building. For this purpose, the object was laser scanned. Object-based parametric modelling was performed from the façade point clouds, and the modelling results were compared to the design documentation.

2. Description of the research performed

2.1. The studied object

The research on the fidelity of mapping glass surfaces and elements from the point cloud in the BIM model was carried out for the glass façade of the building (segments B and C), located in Kraków at Balicka street, formerly the structures of a historic granary (Fig. 1). In 2018, the historic building was revitalized, in order to adapt it to functional use (Fig. 2). Along the eastern façade of the livestock building and warehouse building, one-story extensions were designed in the form of load-bearing steel skeletons with fully glazed walls, with a joinery system (Fig. 3). In order to maintain the character of the existing metal joinery, the Aluprof MB-70 INDUSTRIAL window system was adopted in the design – this particular version is specifically targeted to the modernization of historic buildings and resembles steel windows in buildings under monument conservation protection.



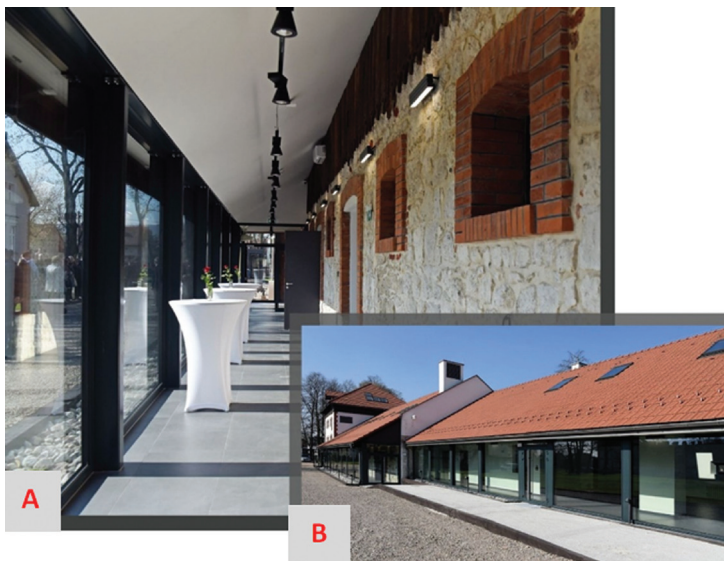
Source: Authors' own study

Fig. 1. View of the east façade of the historic granary, glazed elements marked



Sources: A – www.modernizacjaroku.org.pl/pl [26.10.2020]; B – www.nac.gov.pl/archiwum-audiowizualne/zasob/ [26.10.2020]; C – G. Wojcieszek [www.krakow.naszemiasto.pl, 26.10.2020]

Fig. 2. Granary building: A – current status, B – Granary as the experimental station of the Jagiellonian University's Agricultural Institute, 1934, C – status before the remodelling

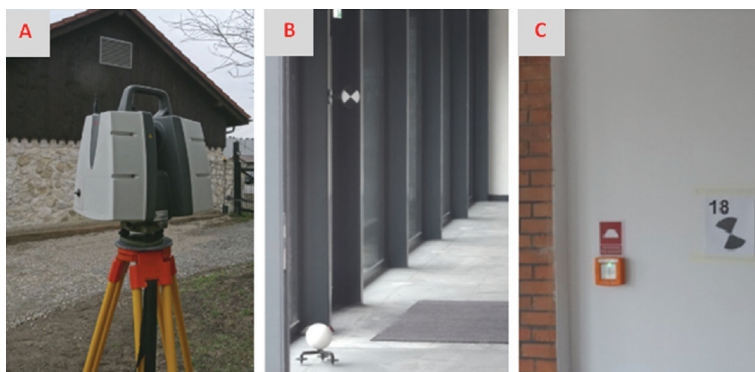


Source: www.lifeinkrakow.pl [26.10.2020]

Fig. 3. Interior of the glazed corridor of the livestock building (A), external appearance (B)

2.2. Terrestrial laser scanning

The survey measurement of the historic granary in the terrestrial laser scanning technology was carried out in March 2019. The laser scanning covered the exterior and the interior of the entire facility, and it took three days. The fieldwork encompassed a total of 12 stations for scanning the exterior façade of the building, and over 70 stations for the interior. The measurement was performed using a Leica ScanStation P40 laser scanner (Fig. 4A). During the measurement, the reference points used for mutual orientation of the scanning stations were metal black-and-white Leica targets, white reference spheres (Fig. 4B), as well as paper black-and-white targets (Fig. 4C), the scanning of which was particularly important in the interior of the building.



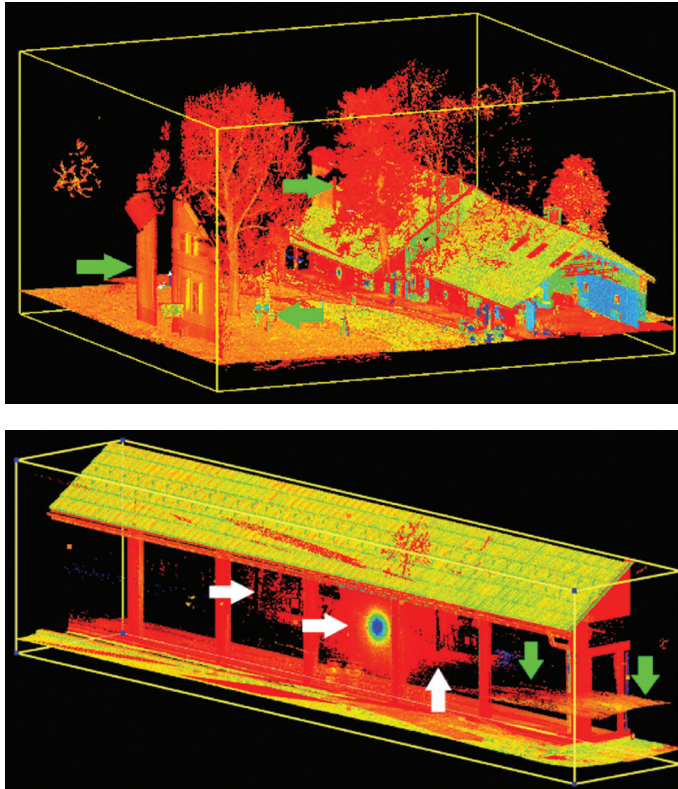
Source: Authors' own study

Fig. 4. TLS measurements: A – Leica ScanStation P40, B – Targets by Leica company and reference spheres, C – Black-and-white targets

The measurement procedure at each station – position of the object's exterior – consisted in conducting two consecutive scans. The first one, performed at low resolution – to the order of 6 cm/20 m (the so-called *preview scan*) – covered the full range of laser visibility and was used to transfer the entire surroundings of the station to 3D space model. Then, within its area, visible from the controller level, the target scanning range of the object was marked, and then the actual scanning was performed with the ultimate resolution of 2 mm/10 m. The interior of the object was scanned in the full panorama of the station, and in the target resolution.

TLS data postprocessing was performed using the Leica Cyclone software application, and it included the registration of point clouds and their manual filtration. The RMS parameter, defining the standard deviation of the relations between the reference points of the given positions, in the development process amounted to 0.001 m. After the modules were registered, the 3D data was manually filtered. The glass façades subjected to modelling had the greatest impact on the amount of noise generated. The curtain wall glazing made of three glass panes increased the disturbance of the laser

beam path. As a result, the cloud model of the object was burdened with noise – the echo of the reflection of objects that do not actually exist in the field (Fig. 5).



Source: Authors' own study

Fig. 5. Cloud of points before filtration was applied

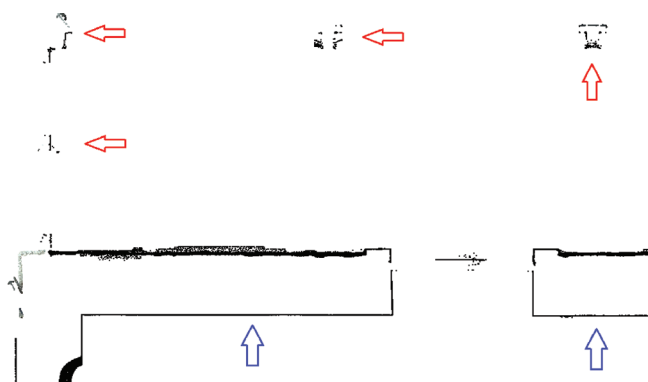
After the filtration process, the object's cloud of points was checked in terms of geometry by making a series of longitudinal and transverse sections. After verifying the geometric correctness of the 3D data, manifested by the continuity of the granary's cloud model, the process of point cloud unification and 5 cm thinning was carried out, which is a standard procedure in the preparation of data for BIM modelling. The last stage of preparing the point cloud for modelling was exporting it to the PTS format.

2.3. Building Information Modelling

The model of the glass façade of the building was developed in the Autodesk Revit software environment, dedicated to Building Information Modelling. The software application is based on parametric object modelling. In order to implement a point

cloud into Revit environment, we first needed to convert the data to the native RCP format. The Autodesk RecCap Pro software application was used for this purpose.

Revit makes it possible to create glazed façades using the curtain wall modelling tools. One of the options is to model a curtain wall using the available systems of elements of this type of walls, which can be modified according to the design needs at any given time. Another way, chosen in this study, is to create a curtain wall from scratch, to divide it into parts using the software's function, and then to manually insert glass joints, constituting the so-called mullions. In the cloud imported to the program, no points forming the glazing surface have been identified. This is due to the fact that the glass is a transparent barrier, and all glass surfaces seemingly mapped by the scanner were necessarily considered false points, therefore they were eliminated during the manual filtration stage in the Leica Cyclone software. Therefore, it was possible to determine the location of the glass façade only on the basis of the visible fragments of the contours – of the columns and the metal window fittings. In the process of modelling the wall, the precise determination of the course of the glass façade on a cloud of points was much more difficult than it would have been in the case of the remaining ones from above (Fig. 6). The blue arrows mark the clearly outlined contours of the brick walls of the building, while the red ones mark parts of the mapped glass façade, which in fact amounts to the outlines, not very clearly visible, of the supporting pillars and fragments of window joinery.

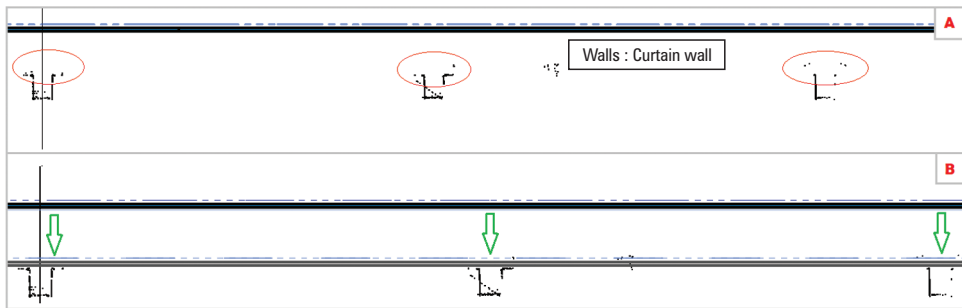


Source: Authors' own study

Fig. 6. Main levels of the buildings: warehouse building (left) and livestock building (right)

The distinction and correct interpretation of the elements visible in the façade cross-section was possible thanks to the prior on-site observations of the facility and the information on the structure included in the design documentation [Miśków-Janik 2017]. After approximate insertion of architectural walls in the line of the columns, their type was changed from the basic wall to the curtain wall. Following this operation, the thickness of the walls changed significantly, which was noticeable in their cross-

sections – the curtain wall, the filling of which is glass, is by design a much narrower partition than standard architectural walls. Therefore, only after changing the partition type, the walls were finally moved with the cursor in order to fit more precisely into the point cloud. The effect of the adjustment is shown in the illustration below (Fig. 7). At this stage of the study, it was assumed that the location of the glass in the line marked by the window joinery (fragments of the cloud marked with a red outline – Fig. 7A) would be the most correct way to recreate its actual course. In order to adjust the glazing of the wall, the fragments best recorded by the scanner were used, and in other places, where the elements of the joinery were not represented well enough, the assumed course of the wall was followed, orthogonal to the view, which was possible thanks to the initial cloud settings in the software application. The places of the beginning and the end of the wall have been set at the edges of the end columns. Both newly created walls were connected at the base and at the top to the previously created levels.



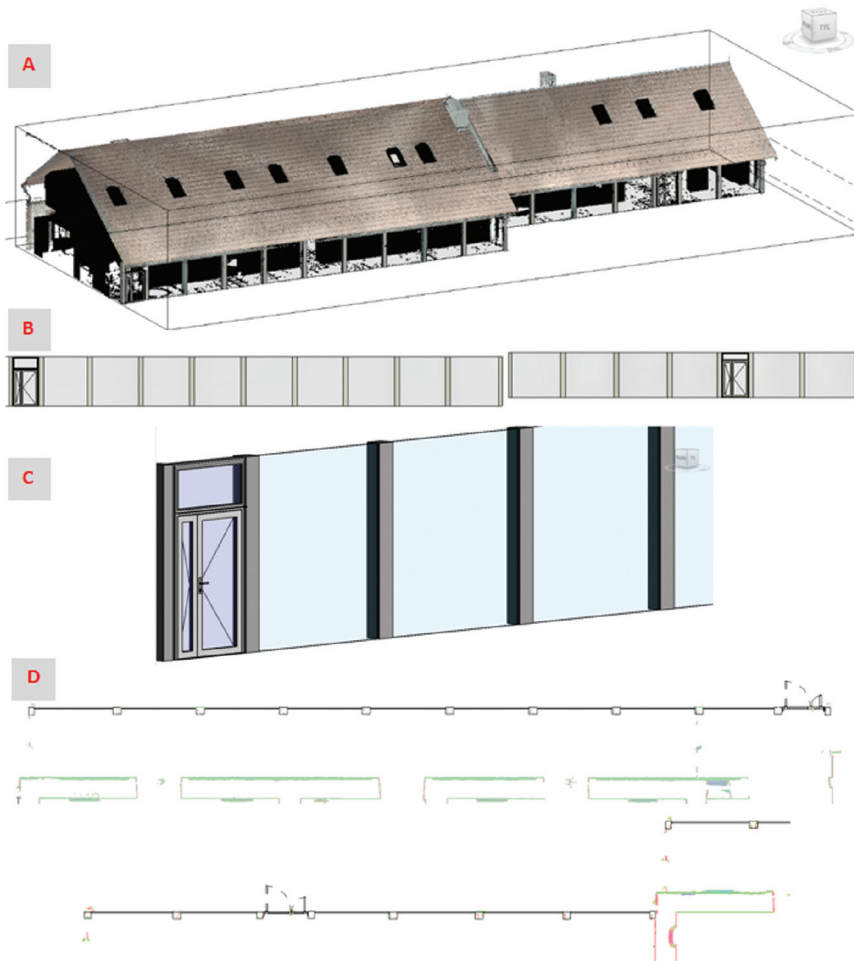
Source: Authors' own study

Fig. 7. Fitting the course of curtain wall glazing to point cloud in cross-section: identification of joinery fragments (A), shifting the wall to its assumed course (B)

The next step in modelling the façade was dividing it into parts using the curtain wall division function. The axes of division are located in the centres of the columns visible on the cloud, using projections and longitudinal sections. The division procedure made it possible to insert mullions within the wall, constituting connections between the glass panes. The purpose of creating the model was to recreate the correct geometry of the building façade from the point cloud, therefore a certain generalization of structural elements and window joinery was necessarily applied: for this purpose, rectangular mullions were inserted in the curtain wall, and then they were modified in such a way that they would include within their bounds the geometry of the supporting columns with window fittings. It was assumed that the axes of the objects modelled in this manner (the correctness of which will be analysed later in the work) would be positioned with the smallest possible error. It should be noted that such an approach to the problem of modelling the façade would not be a correct solution from the building construction point of view, because the mullions of the curtain walls do not consti-

tute a load-bearing structure, and therefore they cannot be equalled with supports (columns). However, for the purposes of recreating the correct geometry of the façade, the present solution was considered sufficient.

The ultimate model of the wall (Fig. 8) was exported to the *IFC 2x3 Coordination View 2.0* format, which is the latest version of the file extension as an open standard. It meets the principle of interoperability by enabling data exchange, ensuring the correct export of all information stored in the original model file, which is one of the most important aspects of working with BIM.



Source: Authors' own study

Fig. 8. Ultimate model: A – 3D view of the modelled glass façades of buildings with point cloud attached, B – View of the modelled glass façades, C – 3D view of the modelled glass façade with the door, D – Projections of the modelled façade (top – livestock building, bottom – warehouse building)

3. Analysis of the results

The BIM model of the glass façade of the building was assessed for the geometrical accuracy of the representation. The wall projections obtained from the design documentation developed for the purpose of remodelling the facility were the reference base for the accuracy analysis. All data pertaining to the object's geometry were included in the documentation in the form of flat drawings, in the digital DWG file format. Therefore, the analysis of the accuracy of reconstructing the façade geometry was performed by comparing the deviations between the projections obtained from the model to those obtained from design data. For this purpose, it was necessary to export the view from the BIM model made in Revit to the DWG format, and then to compare the linear dimensions, after importing the files to Autocad (Autodesk) software application.

Geometric deviations were identified by means of superimposing the projections and sections in the design and in the model. The base point (fit) between the drawings in the case of the projection of the curtain wall of the livestock building was the front of one of the columns and its axis, which marks the longer side of the wall. The choice was made due to the fact that this was the best-reproduced element of this part of the façade. The façade of the warehouse building was adjusted to the geometry of two columns: the initial and the final one, because their outlines were clearly matched with the design documentation. Additionally, the fit of the wall sections covered by the modelling was subjected to comparison.

The accuracy of the reconstruction of the object's geometry was assessed on the basis of the differences in the measured lengths of the segments between the axes of adjacent columns on the projection from the design documentation and the corresponding values on the projection of the developed model.

The analysis was carried out separately for the façade of the livestock building (Fig. 1B) and the façade of the warehouse building (Fig. 1C). The calculations were conducted for 16 segments: 9 in the warehouse building, and 7 in the livestock building. One of the segments was excluded from the calculations – because of the dimension difference computed in its case it differed significantly from the other values, therefore the data of this particular segment was classified as a gross error. The inclusion of the corresponding value would significantly diminish the reliability of the obtained results. The accuracy of the differences between the model's dimensions and design values was assessed by calculating the mean error of a single difference. The computation process was as follows:

(A) Calculation of differences in the measured distances between the axes of the columns:

$$R_i = |P_i - M_i| \quad (1)$$

where:

P_i – the distance between the axes of adjacent columns in the design,

M_i – the distance between the axes of adjacent columns in the model.

(B) Calculation of the arithmetic mean of the measurement differences:

$$\bar{x} = \frac{\sum_{i=1}^n R_i}{n} \tag{2}$$

where:

n – the number of sections for which the differences were calculated.

(C) Calculation of apparent errors of individual measurement differences:

$$v_i = \bar{x} - R_i \tag{3}$$

(D) Calculation of the mean error of the measurement differences:

$$m_0 = \pm \sqrt{\frac{[vv]}{n-1}} \tag{4}$$

where:

$[vv]$ – the sum of squares of apparent errors v_p ,

n – the number of segments for which the differences were calculated.

(E) Calculation of the mean error of the arithmetic mean of the measurement differences:

$$m_x = \pm \sqrt{\frac{[vv]}{n(n-1)}} \tag{5}$$

where:

$[vv]$ – the sum of squares of apparent errors v_p ,

N – the number of segments for which the differences were calculated.

(F) Summary of calculation results:

Table 1. Summary of calculation results for the curtain wall of the livestock building

| Livestock building | | | | | | | |
|--------------------|--------------|--------------|---------------|---------------|-----------------------------|------------------------------------|-----------|
| No. ($n = 9$) | P_i [m] | M_i [m] | P_i [mm] | M_i [mm] | $R_i = P_i - M_i $ [mm] | $v_i = \bar{x}_{Ri} - R_i$ [mm] | vv |
| 1 | 1.629 | 1.694 | 1694 | 1629 | 65 | -45.4 | 2065.1980 |
| 2 | 2.935 | 2.894 | 2894 | 2935 | 41 | -21.4 | 459.8642 |
| 3 | 2.900 | 2.930 | 2900 | 2930 | 30 | -10.4 | 109.0864 |
| 4 | 2.940 | 2.930 | 2940 | 2930 | 10 | 9.6 | 91.3086 |
| 5 | 2.940 | 2.930 | 2940 | 2930 | 10 | 9.6 | 91.3086 |
| 6 | 2.940 | 2.930 | 2940 | 2930 | 10 | 9.6 | 91.3086 |
| 7 | 2.920 | 2.930 | 2920 | 2930 | 10 | 9.6 | 91.3086 |
| 8 | 2.930 | 2.930 | 2930 | 2930 | 0 | 19.6 | 382.4198 |

Table 1. cont.

| Livestock building | | | | | | | |
|---|--------------|--------------|---------------|---------------|-----------------------------|------------------------------------|-----------|
| No. ($n = 9$) | P_i [m] | M_i [m] | P_i [mm] | M_i [mm] | $R_i = P_i - M_i $ [mm] | $v_i = \bar{x}_{Ri} - R_i$ [mm] | νv |
| 9 | 2.930 | 2.930 | 2930 | 2930 | 0 | 19.6 | 382.4198 |
| 10 | 3.005 | 2.774 | 3005 | 2774 | 231 | -211.4 | 44708.750 |
| Total | | | | | 176 | 0.0 | 3764.2220 |
| Mean | | | | | 19.56 | | |
| Maximum | 2.9400 | 2.9350 | 2940 | 2935 | 65 | 45.4 | |
| Minimum | 1.6940 | 1.6290 | 1694 | 1629 | 0 | 9.6 | |
| Mean error of individual measurement difference m_o : | | | | | | | 21.7 mm |
| Mean error of the arithmetic mean m_x : | | | | | | | 7.2 mm |

Source: Authors' own study and data from the project by Miśków-Janik [2017]

Table 2. Summary of calculation results for the curtain wall of the warehouse building

| Warehouse building | | | | | | | |
|---|--------------|--------------|---------------|---------------|-----------------------------|------------------------------------|-----------|
| No. ($n = 9$) | P_i [m] | M_i [m] | P_i [mm] | M_i [mm] | $R_i = P_i - M_i $ [mm] | $v_i = \bar{x}_{Ri} - R_i$ [mm] | νv |
| 11 | 3.050 | 3.060 | 3050 | 3060 | 10 | 20.3 | 411.5102 |
| 12 | 3.040 | 3.055 | 3040 | 3055 | 15 | 15.3 | 233.6531 |
| 13 | 3.060 | 3.055 | 3060 | 3055 | 5 | 25.3 | 639.3673 |
| 14 | 3.055 | 3.040 | 3040 | 3055 | 15 | 15.3 | 233.6531 |
| 15 | 1.716 | 1.615 | 1716 | 1615 | 101 | -70.7 | 5000.5100 |
| 16 | 2.880 | 2.940 | 2880 | 2940 | 60 | -29.7 | 882.9388 |
| 17 | 3.100 | 3.101 | 3100 | 3106 | 6 | 24.3 | 589.7959 |
| Total | | | | | 212 | 0.0 | 7991.4290 |
| Mean | | | | | 30.3 | | |
| Maximum | 3.100 | 3.106 | 3100 | 3106 | 101 | 70.7 | |
| Minimum | 1.716 | 1.615 | 1716 | 1615 | 5 | 15.3 | |
| Mean error of individual measurement difference m_o : | | | | | | | 37.2 mm |
| Mean error of the arithmetic mean m_x : | | | | | | | 14.1 mm |

Source: Authors' own study and data from the project by Miśków-Janik [2017]

As a result of the calculations, the mean error value of a single measurement difference (m_0) was obtained at the level of 21.7 mm for the livestock building, and 37.2 mm for the measurement of the warehouse building. The mean errors of the mean arithmetic measurement differences (m_x) were 7.2 mm and 14.1 mm, respectively. Based on the values obtained, it was found that the level of accuracy of mapping the façades was slightly lower in the case of the warehouse building. However, the assessment should take into account the fact that there was one gross error recorded in the measurement of the first building. After excluding it from the calculations, it was found that its value was more than ten times greater than the calculated mean error of the other differences. The reason for the occurrence of such a substantial inaccuracy could have been a misinterpretation of the point cloud of the last column. The measurement data at this point was inconclusive and incomplete. This may have been due to the infallible removal of some points at this stage of the filtration process. Such a substantial error in the case of measuring the distance was significant as it concerned a corner column of a curtain wall, and thus a boundary column within the model – therefore, it was crucial in the context of measuring the length of the entire modelled façade. According to the data from the design, this dimension is 28.09 m, and in the case of the model it is as much as 28.31 m, which is an unacceptable level of discrepancy. In the case of the livestock building, the mean measurement error was slightly lower, however, it should be noted that the length of the entire façade was modelled flawlessly, at 20.08 m. In addition to the data on the length of the façades, the differences in the height of the curtain walls were also compared – by matching the wall sections obtained from the model with sections from the design documentation. In the case of the livestock building, the height of the wall in the model coincided with the corresponding dimension in the design, and was 2.84 m. This value was measured in accordance with the assumptions of the study – from the floor surface to the location of the transverse structural beam of the wall. From the outside of the building, the wall structure has a different vertical dimension, because its height is defined by the window joinery of the glazed surfaces, and in the case of the livestock building, according to the design data, that height is 3.05 m. Measuring this dimension with a scanner was not possible, because the lower part of the metal fittings is located partly below the gravel surface. The cross-sections also show the width of the supports, modelled in accordance with the assumptions adopted for the purposes of this study, in such a way that they included the outline of both the geometry of the column and the window joinery in the projection. As can be seen from the drawing, the transverse geometry of the supports in the case of the warehouse building is consistent with the design data, and this dimension is 0.24 m in total. For the warehouse building, the dimensions of the wall obtained from the model are as follows: height from the floor level to the crossbeam is 2.53 m, and the width of the supports' outline is 0.24 m. The dimension corresponding to the wall height in the design is 2.54 m, therefore the measurement discrepancy was 20 mm, while in the case of the width, the two measurements coincide. The design height, defined as the dimension of the window joinery in the warehouse building, is 2.73 m. Also in this building, a small part of the glazing frame is below the pavement level. The data is summarized in the table below (Table 3).

Table 3. Juxtaposition of differences in the measurements of height and width of curtain wall supports

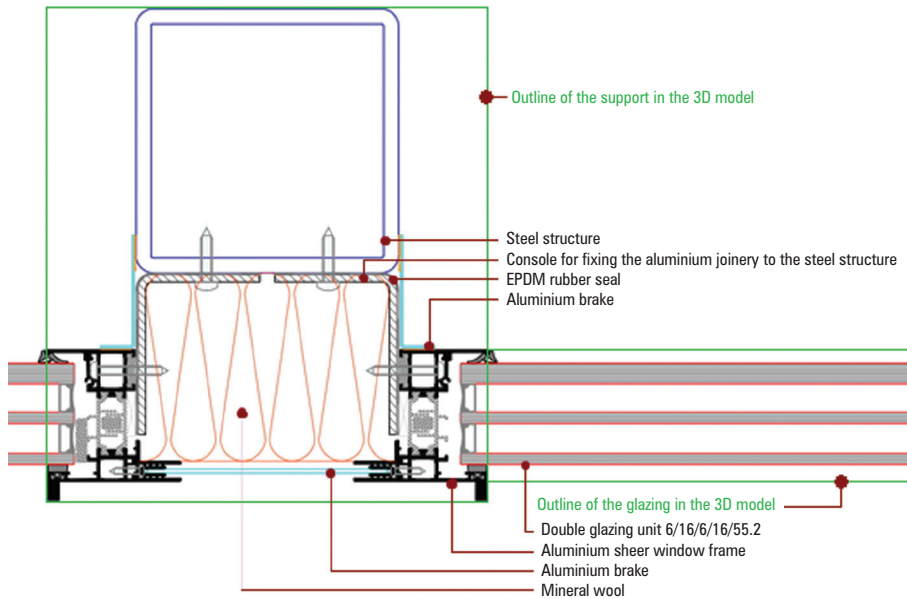
| | Height of the wall assumed as height of the columns [m] | | | Width of the supports [m] (joinery + column) | | | Height of the window joinery designed in the design [m] |
|--------------------|---|--------|------------|--|-----------------------|------------|---|
| | Model | Design | Difference | Model | Design | Difference | |
| Livestock building | 2.84 | 2.84 | 0.00 | 0.24 | 0.24 (0.10 + 0.14) | 0.00 | 3.05 |
| Warehouse building | 2.53 | 2.52 | 0.01 | 0.24 | 0.24 (0.10 + 0.14) | 0.00 | 2.73 |

Source: Authors' own study and data from the project by Miśków-Janik [2017]

The identification of the glass pane in the curtain wall in this study was made on the basis of a point cloud of the window joinery fragments and columns. The pane was fitted based on projections, positioning it centrally against the parts of the metal joinery best mapped by the scanner, and assuming its width as the thickness of the glazing in the model. The value obtained after measuring the point cloud in several places was averaged, and the result was 68 mm, which turned out to be very close to the actual dimension – because according to the design data, this measures 70 mm. As it results from the documentation, the total thickness of the glass pane itself, which is a double glazed unit, is 53.8 mm. The final thickness of the glazing adopted in the model differs from the design value by only 14.2 mm, which is a satisfactory result in terms of accuracy. The applied attempt to interpolate this value, consisting in adjusting the glazing outline to the width of the window frame, was considered to be the most accurate method of reproducing its actual size and foundation. The idea behind such an approach to the modelling of glass panes is presented in the diagram presented below (Fig. 9). The diagram was drafted based on the detail showing the connection of the window joinery with the load-bearing structure, obtained from the design documentation.

As follows from the analyses presented above, when using the adopted approach in the modelling of a curtain wall, the correctness of recreating the geometry of the object produced in glass technology mainly depends on the level of accuracy with which the elements constituting the façade skeleton were measured, in this case steel columns and aluminium window joinery. These elements, depending on their size and the material from which they were made, may also be registered in a way that is difficult to identify in a point cloud, or they may be reproduced with errors resulting from distortions and noise. In the modelled curtain wall, these objects were reproduced with sufficient accuracy, except for the one spot where the gross error was made. However, it was assumed that as a result of scanning performed with high resolution – to the order of 2 mm/10 m – the elements of the wall structure should have been registered in very high quality. The modelling accuracy could also be impacted by the adopted level of unification and thinning of the point cloud – at the level of 5 cm. However, this operation was necessary due to the large size of the files containing the data recorded with such high

resolution. The adopted level of unification is an accepted norm in the development of BIM models. It was also observed that in the case of the cloud of points for some elements of the object, such as brick walls and the roof, the surfaces were very precisely mapped. For this reason, it should be assumed that the imperfections visible in the cloud of points for the columns and the joinery were caused to a greater extent by the specific properties of these elements and by the large surface of glass than by the equipment used, or the level of unification of the measurement data applied.



Source: Authors' own study and data from the project by Miśków-Janik [2017]

Fig. 9. Cross-section of the curtain wall structure and the adopted scheme of modelling

The accuracy of modelling the existing objects using the BIM technology can be determined by LOAs (levels of accuracy), which are defined in two aspects: measurement with the technology used, and representation with the selected tool. According to the manufacturer, the scanner used for measuring ensures the accuracy of the 3D position measurement at the level of 3 mm at 50 metres, and 6 mm at 100 metres. The parameters of the performed recording of the positions are also important – the RMS parameter was 1 mm. It can be assumed that the listed values remain within the scope of the LOA 40 accuracy level, which according to [USIBD 2019] standards falls within the range of 1–5 mm and is the fourth level of accuracy, out of five possible. Therefore, it should be concluded that the accuracy of the measurement was very high indeed. The level of accuracy of the representation – in this case the BIM model – assuming that the real geometry of the object is determined by the design data, on the basis of the calculations performed, was established as LOA 20, determined in the range of 15–50 mm.

4. Conclusions

Building information modelling is a technology that has revolutionized the approach to the design of buildings, construction works management, and the investment process. It enables the development of consistent documentation and making better design decisions, and is the basis for a variety of analyses related to the building and its management, also after the completion of the construction process. The combination of terrestrial laser scanning technology with BIM tools enables the use of the concept of digital object information modelling also in the context of pre-existing objects. As projected by Anna Tryfon-Bojarska, innovation manager of the SKANSKA CDE group, which is a world leader in the construction industry: 'In the perspective of 2025, a lot will change in the implementation of real estate development and construction projects. It will be important to digitize the process throughout the project life cycle, and to create digital twins of physical buildings enabling data analytics' [Autodesk Report 2019]. Photogrammetric measurement techniques play a key role in the virtual architectural reconstruction, and one of those techniques is terrestrial laser scanning. The quality of the 3D model of the existing object, developed in BIM technology, depends on the accuracy and reliability of the measurement works performed, on the correct selection of the scanning instrument in terms of its type and parameters, and on the layout of the measurement stations, as well as on the appropriate selection of the scanning resolution. It is also important to correctly interpret the measurement data, and to make sure that they are processed properly and reliably, with the use of appropriately selected methods and software applications. TLS technology also brings with it measurement limitations that cannot be controlled, as they result from the specificity of scanning various materials. Glass is undoubtedly one such a material, which is increasingly used in construction. The combination of BIM tools with laser scanning data, which is the research aspect of this article, provided satisfactory solutions in terms of the possibility of recreating the geometry of objects made in glass technology. Properly interpreted and processed data obtained from scanning, in integration with BIM object-oriented parametric modelling, enable inventorying of complex and problematic structures. By supplementing the model made in this way with an information layer, it is possible to develop a comprehensive, virtual database reflecting the actual condition of objects.

Funded from a subsidy by the Ministry of Education and Science for the University of Agriculture in Krakow for the year 2021.

References

- Alshawabkeh Y., Baik A., MikyY. 2021. Integration of Laser Scanner and Photogrammetry for Heritage BIM Enhancement. ISPRS International Journal of Geo-Information, 10(5), 316.
- Autodesk. 2019. Budownictwo. Innowacje. Wiza liderów branży 2025 – raport wykonany przez firmę ASM. Centrum Badań i Analiz Rynku.
- Baik A. 2017. From point cloud to jeddah heritage BIM nasif historical house – case study. Digital Applications in Archaeology and Cultural Heritage, 4, 1–18.

- Głowacka A., Pluta M. 2015. Dokładność modelowania 3D na podstawie chmury punktów z naziemnego skaningu laserowego. *Episteme*, 26(2), 125–132.
- Graham K., Chow L., Fai S. 2018. Level of detail, information and accuracy in building information modelling of existing and heritage buildings. *Journal of Cultural Heritage Management and Sustainable Development*.
- Kamusiński A. 2005. Refleksje na temat zjawisk fizycznych związanych z ruchem ciał w przestrzeni. *Zeszyty Naukowe Akademii Marynarki Wojennej*, 46, 13–74.
- Kelly G., Serginson M., Lockley S., Dawood N., Kassem M. 2013. BIM for facility management: A review and a case study investigating the value and challenges. *Proceedings of the 13th International Conference on Construction Applications of Virtual Reality*, 5.
- Khosakitchalert C., Yabuki N., Fukuda T. 2019. Improving the accuracy of BIM-based quantity takeoff for compound elements. *Automation in Construction*, 106, 102891.
- Kusznier J. 2015. Początki techniki światłowodowej. *Zeszyty Naukowe Wydziału Elektrotechniki i Automatyki Politechniki Gdańskiej*.
- Kuzina E., Rimshin V. 2017. Deformation monitoring of road transport structures and facilities using engineering and geodetic techniques. In: *Energy Management of Municipal Transportation Facilities and Transport*. Springer, Cham, 410–416.
- Kwinta A., Gradka R. 2021. Dynamic objects geometry measurement by laser scanning – a case study. *Geomatics, Landmanagement and Landscape*.
- Miśków-Janik E. 2017. Przebudowa i rozbudowa budynków Uniwersytetu Rolniczego wraz ze zmianą sposobu użytkowania budynków gospodarczych na potrzeby dydaktyczne oraz stołówki studenckiej wraz z instalacjami wewnętrznymi przy ul. Balickiej 253b w Krakowie na działce nr 15/4 obr. 48 Kraków (dokumentacja projektowa obiektu badań).
- Piech I., Kwoczynska B., Slowik D. 2018. Using Terrestrial Laser Scanning in Documentation of Antique Vehicles. 2018 Baltic Geodetic Congress (BGC Geomatics). *IEEE*, 373–376.
- Pitkänen T.P., Raumonon P., Liang X., Lehtomäki M., Kangas A. 2021. Improving TLS-based stem volume estimates by field measurements. *Computers and Electronics in Agriculture*, 180, 105882.
- Pu S., Vosselman G. 2007. Extracting windows from terrestrial laser scanning. *Intl Archives of Photogrammetry, Remote Sensing and Spatial Information Sciences*, 36, 12–14.
- Yang H., Xu X., Neumann I. 2019. An automatic finite element modelling for deformation analysis of composite structures. *Composite Structures*, 212, 434–438.

Mgr inż. Marta Wider
University of Agriculture in Krakow
Faculty of Environmental Engineering and Land Surveying
e-mail: martawider17@gmail.com

Dr inż. Pelagia Gawronek
University of Agriculture in Krakow
Department of Land Surveying
ul. Balicka 253, 30-198 Kraków
e-mail: pelagia.gawronek@urk.edu.pl
ORCID: 0000-0001-7806-909X